

## Near-infrared enhanced carbon nanodots by thermally assisted growth

Xiaoming Wen, Pyng Yu, Yon-Rui Toh, Yu-Chieh Lee, An-Chia Hsu, and Jau Tang

Citation: [Applied Physics Letters](#) **101**, 163107 (2012); doi: 10.1063/1.4760275

View online: <http://dx.doi.org/10.1063/1.4760275>

View Table of Contents: <http://scitation.aip.org/content/aip/journal/apl/101/16?ver=pdfcov>

Published by the [AIP Publishing](#)

---

### Articles you may be interested in

[Luminescent carbon quantum dots with high quantum yield as a single white converter for white light emitting diodes](#)

Appl. Phys. Lett. **107**, 213102 (2015); 10.1063/1.4936234

[Room-temperature near-infrared silicon carbide nanocrystalline emitters based on optically aligned spin defects](#)

Appl. Phys. Lett. **105**, 243112 (2014); 10.1063/1.4904807

[Enhancement of photoluminescence from defect states in ZnS random photonic crystal: An effect of electronic and photonic mode coupling](#)

J. Appl. Phys. **115**, 043105 (2014); 10.1063/1.4862927

[Near-infrared fluorescent single walled carbon nanotube-chitosan composite: Interfacial strain transfer efficiency assessment](#)

Appl. Phys. Lett. **102**, 171903 (2013); 10.1063/1.4803938

[Strong visible and near-infrared electroluminescence and formation process in Si-rich polymorphous silicon carbon](#)

J. Appl. Phys. **111**, 053108 (2012); 10.1063/1.3691904

---

A promotional banner for Applied Physics Reviews. On the left is a small image of a journal cover for 'Applied Physics Reviews' featuring a diagram of a layered structure. The main background is blue with a glowing light effect. The text 'NEW Special Topic Sections' is prominently displayed in white. Below this, it says 'NOW ONLINE' in yellow, followed by 'Lithium Niobate Properties and Applications: Reviews of Emerging Trends' in white. The AIP Applied Physics Reviews logo is in the bottom right corner.

**NEW Special Topic Sections**

**NOW ONLINE**  
Lithium Niobate Properties and Applications:  
Reviews of Emerging Trends

**AIP** Applied Physics  
Reviews

## Near-infrared enhanced carbon nanodots by thermally assisted growth

Xiaoming Wen,<sup>a)</sup> Pyng Yu, Yon-Rui Toh, Yu-Chieh Lee, An-Chia Hsu, and Jau Tang<sup>a)</sup>  
*Research Center for Applied Sciences, Academia Sinica, Taipei, Taiwan*

(Received 22 July 2012; accepted 3 October 2012; published online 18 October 2012)

The near-infrared emission, matching the biological window, is conducive to biological applications. To date, most of the reported carbon nanodots emit the blue to green fluorescence and few of carbon nanodots emit the near-infrared with relatively lower efficiency. Here, we report an approach to generate or to enhance the near-infrared luminescence from the green luminescent carbon nanodots. Experiments reveal that the near-infrared emission is significantly enhanced by thermally assisted growth in vacuum, which is attributed to the formation of the larger nano-domains from the small carbon clusters at elevated temperatures. © 2012 American Institute of Physics. [<http://dx.doi.org/10.1063/1.4760275>]

Carbon nanodots (CNDs) belong to a kind of luminescent carbon nanoparticles that consist of a graphite structure or an amorphous carbon core and carbonaceous surface.<sup>1-4</sup> In recent years, CNDs have attracted remarkable research interest due to their unique optical properties, huge availability, and nontoxicity and thus great potential applications in bioimaging, photonics, and photocatalysis.<sup>2-9</sup> In particular, CNDs offer promising perspective as an alternative to organic dyes and semiconductor quantum dots (QDs) in bioimaging and biosensor applications.<sup>10</sup> The poor photostability of organic dyes restrains further applications. Semiconductor QDs have attracted extensive attention to replace the organic dyes as bioimaging agents due to their superior optical properties, such as tunable emission, high efficiency, and broad excitation.<sup>11</sup> However, heavy metals in the QDs can lead to serious problems, such as biotoxicity. In contrast, CNDs have emerged as one of the most prospective alternatives to replace QDs based on transitional heavy metal in bioimaging and medical diagnostics because of their biocompatible, nontoxic, excellent chemical- and photo-stabilities as well as superior optical properties, including tunable photoluminescence (PL), non-blinking, and high efficiency.<sup>1,6,7,12</sup>

In recent years, various synthesis techniques have been developed, such as fragmentation/fractionation of suitable carbon sources followed by surface passivation or alternatively by bottom-up strategies utilizing molecular precursors, and simple techniques such as combustion, thermal, or microwave treatments.<sup>1,8,13</sup> To date, most of the reported CNDs emit the blue to green fluorescence, and they usually exhibit excitation wavelength dependent PL.<sup>7,12,14-17</sup> Near-infrared (NIR) materials are promising labeling reagents for sensitive determination and imaging of biological targets because of much lower absorption and minimal cellular auto-fluorescence, thus, low background and large penetration depth.<sup>18</sup> Unfortunately, few CNDs were reported for the red or NIR emission with relatively low efficiency.<sup>6,13</sup> Extending the PL to match NIR window of biological tissue will greatly facilitate the biological applications of CNDs.<sup>18</sup>

Here, we report an approach to significantly enhance the NIR PL from the green luminescent CNDs by thermally

assisted growth. By monitoring the PL evolution of the CNDs, it is found that the original green PL basically remains unchanged and a NIR emission band gradually increases during the growth at an elevated temperature. The NIR band is ascribed to the thermally assisted formation of the larger sp<sup>2</sup> nano-domains.

The carbon nanodots used in this study were synthesized using a simple bottom-up approach developed by Fang *et al.*<sup>4</sup> Briefly speaking, a mixture solution of 1 ml glacial acetic acid and 80  $\mu$ l H<sub>2</sub>O was quickly added to 2.5 g of P<sub>2</sub>O<sub>5</sub> with the spontaneous heat. The carbon dots were collected by dispersing into 5 ml DI water for further optical measurements. It has been identified that as-synthesized CNDs have small sp<sup>2</sup> nano-domains that result in the fluorescent emission at 530 nm.<sup>1,4,17</sup> It should be noted that such CNDs consist of abundant carboxylic group, thus, they exhibit excellent solubility for the biologic applications. The CNDs film was fabricated by conventional drop casting on substrate of glass. The substrate was under careful ultrasonic cleaning for 1 h. Then, it was processed for hydrophilicity in sulphuric acid for 2 h and stored in vacuum for drying. After drop casting, the film was stored in vacuum. The film was fixed in a cryostat at controllable temperature in vacuum for at least 1 h before increasing temperature in order to evacuate oxygen. A CCD equipped spectrometer (HORIBA Jobin Yvon) was used to monitor the PL evolution at excitation of 406 nm. The lifetimes were measured by time correlated single photon counting (TCSPC) in Microtime-200 system (Picoquant) with an excitation of 467 nm laser.

Figure 1(a) shows the absorption and PL spectra of the CNDs. Similar to the observation by others, the absorption peak at 300 nm is ascribed to n- $\pi^*$  transition of C=O bands and that of 250 nm was attributed to  $\pi - \pi^*$  transition of aromatic C=C bonds.<sup>19</sup> It was observed that the PL of the film exhibits a red shift of 10 nm with respect to that of the solution, which is usually attributed to electron or energy transfer within the inhomogeneous distribution emitting species within the solid film and probably inner filter effects.<sup>20,21</sup> The PL is found to be excitation-wavelength dependent with the peak located at 530 nm in solution excited at 406 nm, similar to the other CNDs.<sup>2</sup> Figure 1(b) shows the image of transmission electron microscopy (TEM). The absorption and PL spectra are essentially similar to that reported by other groups.<sup>4</sup>

<sup>a)</sup>Authors to whom correspondence should be addressed. Electronic addresses: [xwen@gate.sinica.edu.tw](mailto:xwen@gate.sinica.edu.tw) and [jautang@gate.sinica.edu.tw](mailto:jautang@gate.sinica.edu.tw).

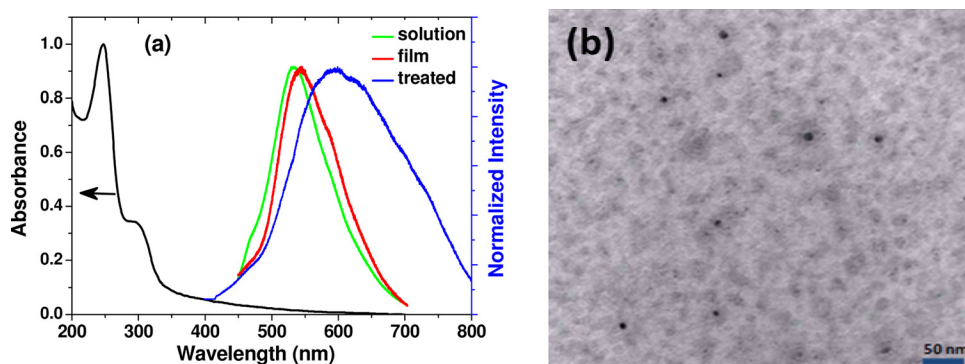


FIG. 1. (a) Absorption and fluorescence spectra of as-synthesized CNDs in aquatic solution, film, and the thermally treated CND film. (b) TEM image of as-synthesized CNDs.

The film was then thermally treated at an elevated temperature. We monitored the PL kinetic process during thermally assisted growth, as shown in Figure 2 for 400 K. It is evident that the PL in the NIR is significantly enhanced upon thermal growth from the initial (black) to the thermal growth (blue) within 1 h. In contrast, the PL spectrum at the green region does not show obvious change. It is interesting to note that a PL band centered at 700 nm generates gradually upon thermal growth, as shown in the dashed line. A PL band can be extracted by subtraction of the initial PL spectrum from that thermal growth for 1 h. It should be noted that the intensity of PL evidently decreases and spectrum slightly broadens in the red side with increasing temperature. This is due to the increased nonradiative trapping, which has been observed in most of luminescent materials. The PL intensity then significantly increases and spectrum basically remains upon naturally cooling from the elevated temperature to room temperature due to decreased nonradiative relaxation.<sup>22</sup>

Figure 3 summarizes the PL intensity evolution (a) at 550, 650, and 700 nm at 400 K and (b) 700 nm at temperature of 400, 420, and 450 K, respectively. Upon thermal growth, the PL spectrum exhibits an evident red shift, due to the generation of emission band in the NIR. With thermal growth, the PL in the NIR increases gradually and the saturation appears around 60 min. At different temperatures, 400, 420, and 450 K, the PL in the NIR essentially exhibits similar tendency such that PL increases gradually and then saturates around 60 min. As shown in Figure 3(b), for thermal growth

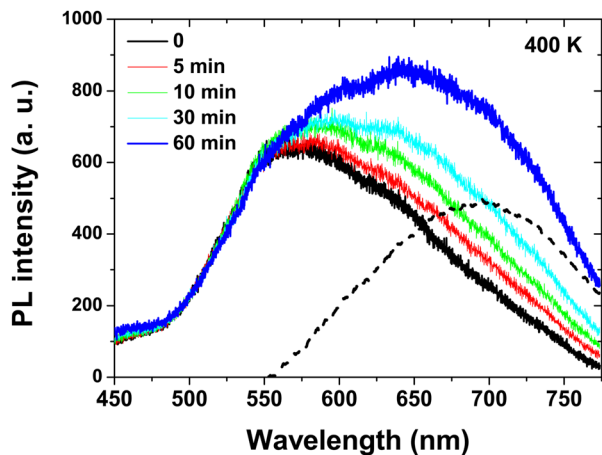


FIG. 2. PL kinetics with thermal growth at 400 K in vacuum. The dashed line represents the newly generated emission extracted by subtracting the initial PL (black line) from the thermally grown sample (blue line) at 60 min.

at 400 K, the PL intensity exhibits a larger enhancement than that at the higher temperature; while the spectrum extension in the NIR does not exhibit obvious difference. For thermally grown samples at 380 K, the extension of PL spectrum is evidently smaller than that at 400 K. It should be noted that during the thermal growth the PL intensity at 550 nm roughly remains stable. After thermal growth, the sample cools naturally in vacuum. It is found that the PL is significantly enhanced at the NIR region with a slightly red shift in the green, as compared in Figure 1.

We performed similar thermally assisted growth for CNDs in  $N_2$ . It is found that a similar effect occurs in  $N_2$  ambient to that in vacuum. It is found that the oxygen is very harmful for the thermal treatment. In ambient oxygen

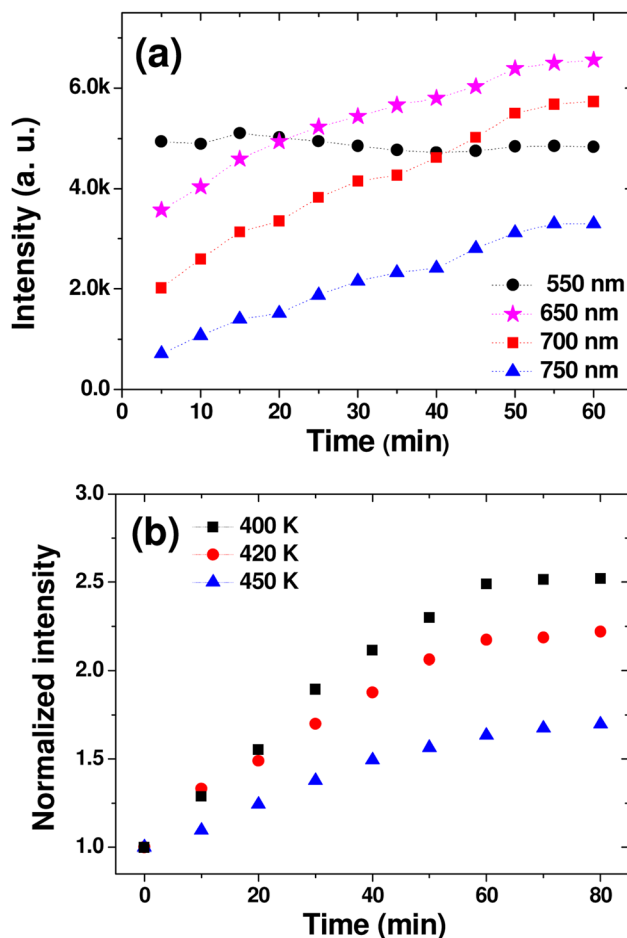


FIG. 3. (a) The PL evolution of CNDs at 550, 650, 700, and 750 nm at 400 K, and (b) PL evolution at 700 nm at 400 K, 420 K, and 450 K, respectively.

presence, the PL spectrum exhibits an evident broadening and the total intensity decreases obviously. It is not surprised because oxygen atoms in air easily react with the CNDs at elevated temperatures. It results in increased defect/surface states, which can act as nonradiative centre to quench the PL. It should be noted that both as-synthesized and thermally treated CNDs exhibit excellent photostability, compared to the commercial CdSe QDs.

To acquire further insight, we measured the lifetimes for as-synthesized and thermally treated CNDs. Figure 4(a) compares the PL evolutions for as-synthesized and thermal growth CNDs at 650 nm. Each sample exhibits biexponential decay, similar to the other observations,<sup>23–25</sup> as summarized by the fitting parameters in Table I. The average lifetime is calculated by  $\tau_{av} = (A_1 \cdot \tau_1 + A_2 \cdot \tau_2)/(A_1 + A_2)$  with  $A_1$  and  $A_2$  the amplitudes of the two lifetime components. The lifetime at 550 nm does not display evident difference, which suggests similar fluorophore or emission mechanism. In contrast, at 650 nm, the thermally treated sample exhibits a significantly increased lifetime, from 0.85 ns to 2.89 ns. This implies significantly decreased nonradiative traps and increased fluorophore density.

Figure 4(b) compares the Raman spectra of as-synthesized and thermally treated CNDs excited at 633 nm. Two evident peaks were assigned to the D band at  $1348 \text{ cm}^{-1}$  and the G band at  $1581 \text{ cm}^{-1}$ . The D and G bands

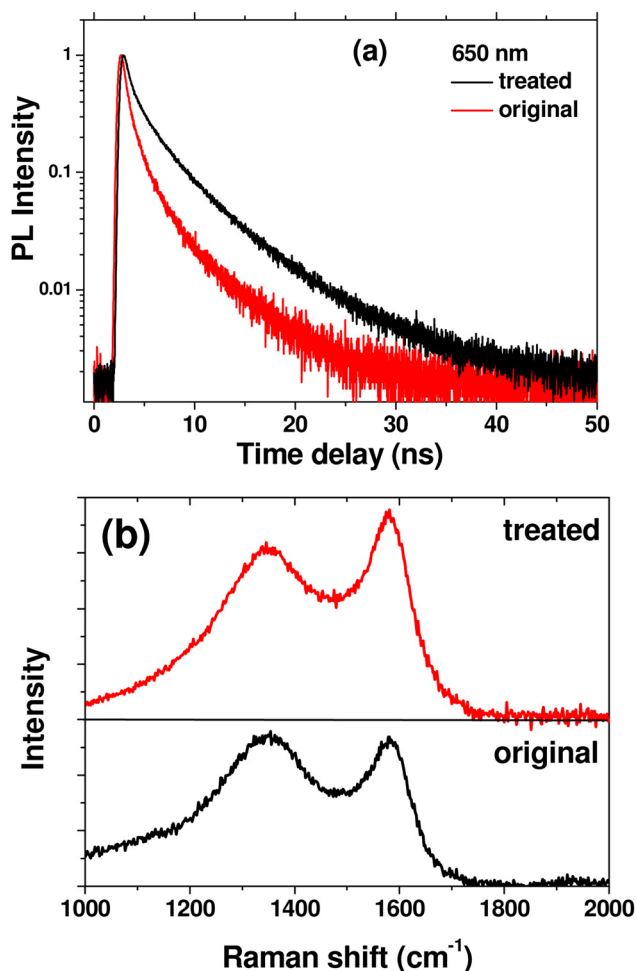


FIG. 4. (a) PL lifetimes at 650 nm and (b) Raman spectra excited at 633 nm of as-synthesized and thermally grown CNDs.

TABLE I. Fitting parameters of PL evolution for as-synthesized and thermally grown CNDs using a biexponential function (lifetime: ns).

	550 nm				650 nm			
	$\tau_1$	%	$\tau_2$	$\tau_{av}$	$\tau_1$	%	$\tau_2$	$\tau_{av}$
As synthesized	0.92	57.9	4.21	2.31	0.52	85.3	2.63	0.85
Thermal growth	0.90	58.4	4.27	2.30	1.00	49.1	4.72	2.89

were studied in disordered and amorphous carbon;<sup>26</sup> intensity of D band is connected to the aromatic rings. The ratio  $I_D/I_G$  was found to be varied inversely with the size of nano domains of aromatic rings and the broadening of the D band is correlated to a distribution of clusters with different orders and dimensions.<sup>27</sup> After thermal treatment, the ratio of  $I_D/I_G$  decreases to 0.814 from original 1.05; this suggests that the treatment results in an increase of the large sized nano domains.

In recent years, the PL of CNDs has been extensively studied.<sup>2,3,7,17,28–30</sup> To date, the detailed PL mechanism has not yet completely understood. Essentially, nano-sized carbon domains and the surface localized states are proposed to be responsible for the observed PL.<sup>31</sup> Eda *et al.* revealed that the size of  $sp^2$  nano-domains determined the emission band gap and thus the emission wavelength.<sup>19,32</sup> Pan *et al.* proposed that the PL may be attributed to free zigzag sites with a carbene-like triplet ground state.<sup>30</sup> Zhu *et al.* suggested that the synergic effect of both zigzag sites and surface defects will determine the emission energy.<sup>33</sup> Krysmann *et al.* studied the formation mechanism of CNDs and argued that the PL of CNDs originates from the surface states localized in edge of  $sp^2$  carbon.<sup>8</sup>

It has been shown that CNDs are generally small oxygenous carbon nanoparticles that are composed of  $sp^2$  carbon atoms hybridized with abundant oxygenous residues, which include small conjugated carbon clusters (aromatic structures) embedded in oxygenous groups.<sup>4</sup> The isolated aromatic structures, also referred as nano-domains, possess suitable band gaps and would generate the visible PL by radiative recombination. The PL of CNDs originates from the recombination of electron-hole pairs, localized within small  $sp^2$  nano-domains that are embedded within a  $sp^3$  matrix.<sup>17</sup> Due to quantum confinement, the emission energy is dependent on the size of the nano-domains; thus, the large-sized nano-domains will be responsible for the NIR emission.<sup>19</sup> It has been known that the size of the CNDs actually cannot determine the energy of PL because usually each CND contains many different  $sp^2$  domains. Isolated  $sp^2$  nano-domains dispersed within the  $sp^3$  matrix can functionalize as PL centers, an effect that is governed by the  $\pi$  states of  $sp^2$  sites. In particular, the PL behavior of amorphous/disordered graphite containing a mixture of  $sp^2$  and  $sp^3$  carbons has been attributed to the radiative recombination of electron-hole pairs that were photo-generated, trapped, and localized within small  $sp^2$  carbon clusters, which are surrounded by  $sp^3$  defects, a mechanism that can remain active in the presence of hetero-atoms.<sup>19,32</sup>

In addition to the size, it is known that the PL band can be influenced by the shape and fraction of  $sp^2$  nano-domains in the  $sp^3$  matrix. Therefore, it is expected that the nano-



domains of larger sizes are essentially responsible for the NIR PL.<sup>25,34</sup> In other words, the NIR PL can be generated/enhanced by forming larger-sized nano-domains. It has been shown that a large amount of carbon fragments are formed during the synthesis of the CNDs.<sup>13,35</sup> During thermal growth, the large nano-domains are thermally assisted to form. At the same time, part of nonradiative defect states can be removed. At elevated temperatures, the carbon fragments obtain an increased thermal energy and readily form the larger nano-domains that are responsible for the NIR emission. This claim is supported by the Raman measurement. Isolated oxygen atoms are conducive to decreasing defect states, usually resulting in nonradiative recombination and quenched PL. However, if the sample is thermally treated in air, oxygen may be adsorbed on the surface, ionized, then implanted into the sample and form some oxygen relevant defects. On the other hand, oxygen atoms may react with carbon atoms in CNDs at the elevated temperature. Furthermore, at the higher treatment temperatures, the interconnectivity of the localized  $sp^2$  nano-domains increases, thereby facilitates hopping of excitons to nonradiative recombination centers, as a consequence, result in quenching PL.

In summary, we have investigated the generation/enhancement of the NIR luminescence from the green luminescent CNDs by thermally assisted growth. The thermally treated CNDs exhibit significantly enhanced NIR fluorescence centered at 700 nm and increased quantum efficiency. This effect is relevant to temperature and the ambient. The NIR band is attributed to the formation of larger  $sp^2$  carbon nano-domains at elevated ambient and decreased nonradiative defect states.

We gratefully acknowledge Dr. Shigeto and Dr. Huang at National Chiao-Tung University for Raman measurement and Instrumental Centre of National Taiwan University for the use of TEM. We also acknowledge the financial support from Academia Sinica (AS) Nano Program and National Science Council (NSC) of Taiwan under Program Nos. 99-2221-E-001-002-MY3 and 99-2113-M-001-023-MY3.

<sup>1</sup>Y. P. Sun, B. Zhou, Y. Lin, W. Wang, K. A. S. Fernando, P. Pathak, M. J. Mezzani, B. A. Harruff, X. Wang, H. F. Wang, P. J. G. Luo, H. Yang, M. E. Kose, B. L. Chen, L. M. Veca, and S. Y. Xie, *J. Am. Chem. Soc.* **128**, 7756–7757 (2006).

<sup>2</sup>S. N. Baker and G. A. Baker, *Angew. Chem., Int. Ed.* **49**, 6726–6744 (2010).

<sup>3</sup>S. Chandra, S. H. Pathan, S. Mitra, B. H. Modha, A. Goswami, and P. Pramanik, *RSC Adv.* **2**, 3602–3606 (2012).

<sup>4</sup>Y. Fang, S. Guo, D. Li, C. Zhu, W. Ren, S. Dong, and E. Wang, *ACS Nano* **6**, 400–409 (2012).

- <sup>5</sup>A. B. Bourlinos, R. Zboril, J. Petr, A. Bakandritsos, M. Krysmann, and E. P. Giannelis, *Chem. Mater.* **24**, 6–8 (2012).
- <sup>6</sup>X. Guo, C. F. Wang, Z. Y. Yu, L. Chen, and S. Chen, *Chem. Commun.* **48**, 2692–2694 (2012).
- <sup>7</sup>H. Z. Zheng, Q. L. Wang, Y. J. Long, H. J. Zhang, X. X. Huang, and R. Zhu, *Chem. Commun.* **47**, 10650–10652 (2011).
- <sup>8</sup>M. J. Krysmann, A. Kelarakis, P. Dallas, and E. P. Giannelis, *J. Am. Chem. Soc.* **134**, 747–750 (2012).
- <sup>9</sup>H. Peng and J. Travas-Sejdic, *Chem. Mater.* **21**, 5563–5565 (2009).
- <sup>10</sup>L. Cao, S. T. Yang, X. Wang, P. G. Luo, J. H. Liu, S. Sahu, Y. Liu, and Y. P. Sun, *Theranostics* **2**, 295–301 (2012).
- <sup>11</sup>M. Bruchez, Jr., M. Moronne, P. Gin, S. Weiss, and A. P. Alivisatos, *Science* **281**, 2013–2016 (1998).
- <sup>12</sup>F. Wang, Z. Xie, H. Zhang, C. Y. Liu, and Y. G. Zhang, *Adv. Funct. Mater.* **21**, 1027–1031 (2011).
- <sup>13</sup>F. Wang, M. Kreiter, B. He, S. Pang, and C. Liu, *Chem. Commun.* **46**, 3309–3311 (2010).
- <sup>14</sup>J. J. Zhou, Z. H. Sheng, H. Y. Han, M. Q. Zou, and C. X. Li, *Mater. Lett.* **66**, 222–224 (2012).
- <sup>15</sup>Z. C. Yang, M. Wang, A. M. Yong, S. Y. Wong, X. H. Zhang, H. Tan, A. Y. Chang, X. Li, and J. Wang, *Chem. Commun.* **47**, 11615–11617 (2011).
- <sup>16</sup>S. T. Yang, L. Cao, P. G. J. Luo, F. S. Lu, X. Wang, H. F. Wang, M. J. Mezzani, Y. F. Liu, G. Qi, and Y. P. Sun, *J. Am. Chem. Soc.* **131**, 11308–11309 (2009).
- <sup>17</sup>S. Srivastava and N. S. Gajbhiye, *ChemPhysChem* **12**, 2624–2632 (2011).
- <sup>18</sup>C. L. Amiot, S. Xu, S. Liang, L. Pan, and J. X. Zhao, *Sensors* **8**, 3082–3105 (2008).
- <sup>19</sup>G. Eda, Y. Y. Lin, C. Mattevi, H. Yamaguchi, H. A. Chen, I. Chen, C. W. Chen, and M. Chhowalla, *Adv. Mater.* **22**, 505–509 (2010).
- <sup>20</sup>O. I. Micic, K. M. Jones, A. Cahill, and A. J. Nozik, *J. Phys. Chem. B* **102**, 9791–9796 (1998).
- <sup>21</sup>S. Crooker, J. Hollingsworth, S. Tretiak, and V. Klimov, *Phys. Rev. Lett.* **89**, 186802 (2002).
- <sup>22</sup>X. Wen, A. Sitt, P. Yu, Y. R. Toh, and J. Tang, *Phys. Chem. Chem. Phys.* **14**, 3505–3512 (2012).
- <sup>23</sup>Y. M. Long, C. H. Zhou, Z. L. Zhang, Z. Q. Tian, L. Bao, Y. Lin, and D. W. Pang, *J. Mater. Chem.* **22**, 5917–5920 (2012).
- <sup>24</sup>X. Wang, L. Cao, S. T. Yang, F. Lu, M. J. Mezzani, L. Tian, K. W. Sun, M. A. Bloodgood, and Y. P. Sun, *Angew. Chem.* **122**, 5438–5442 (2010).
- <sup>25</sup>T. Gokus, R. Nair, A. Bonetti, M. Bohmler, A. Lombardo, K. Novoselov, A. Geim, A. Ferrari, and A. Hartschuh, *ACS Nano* **3**, 3963–3968 (2009).
- <sup>26</sup>F. Tuinstra and J. L. Koenig, *J. Chem. Phys.* **53**, 1126 (1970).
- <sup>27</sup>A. Ferrari and J. Robertson, *Phys. Rev. B* **61**, 14095 (2000).
- <sup>28</sup>J. Peng, W. Gao, B. K. Gupta, Z. Liu, R. Romero-Aburto, L. H. Ge, L. Song, L. B. Alemany, X. B. Zhan, G. H. Gao, S. A. Vithayathil, B. A. Kaiparettu, A. A. Marti, T. Hayashi, J. J. Zhu, and P. M. Ajayan, *Nano Lett.* **12**, 844–849 (2012).
- <sup>29</sup>L. Cao, X. Wang, M. J. Mezzani, F. S. Lu, H. F. Wang, P. J. G. Luo, Y. Lin, B. A. Harruff, L. M. Veca, D. Murray, S. Y. Xie, and Y. P. Sun, *J. Am. Chem. Soc.* **129**, 11318–11319 (2007).
- <sup>30</sup>D. Pan, J. Zhang, Z. Li, and M. Wu, *Adv. Mater.* **22**, 734–738 (2010).
- <sup>31</sup>L. Tang, R. Ji, X. Cao, J. Lin, H. Jiang, X. Li, K. S. Teng, C. M. Luk, S. Zeng, and J. Hao, *ACS Nano* **6**, 5102–5110 (2012).
- <sup>32</sup>K. P. Loh, Q. Bao, G. Eda, and M. Chhowalla, *Nat. Chem.* **2**, 1015–1024 (2010).
- <sup>33</sup>S. Zhu, J. Zhang, X. Liu, B. Li, X. Wang, S. Tang, Q. Meng, Y. Li, C. Shi, and R. Hu, *RSC Adv.* **2**, 2717–2720 (2012).
- <sup>34</sup>Z. Liu, J. T. Robinson, X. Sun, and H. Dai, *J. Am. Chem. Soc.* **130**, 10876–10877 (2008).
- <sup>35</sup>S. Hu, Y. Guo, Y. Dong, J. Yang, J. Liu, and S. Cao, *J. Mater. Chem.* **22**, 12053–12057 (2012).